ACS Medicinal Chemistry Letters

Letter

pubs.acs.org/acsmedchemlett

A Structurally Simplified Analogue of Geldanamycin Exhibits Neuroprotective Activity

Manikandadas M. Madathil,[†,‡] Omar M. Khdour,[†] Jennifer Jaruvangsanti,[†,‡] and Sidney M. Hecht*[,†,‡]

[†]Center for BioEnergetics, Biodesign Institute, and [‡]Department of Chemistry and Biochemistry, Arizona State University, Tempe, Arizona 85287-2904, United States

Supporting Information

ABSTRACT: The syntheses of a structurally simplified geldanamycin analogue **2** and two related compounds are described. Compound **2** conferred cytoprotection and quenched ROS and lipid peroxidation in a dose-dependent manner in Friedreich's ataxia (FRDA) lymphocytes at low micromolar concentrations. It also prevented ROS-induced damage of cellular lipid membranes and maintained the mitochondrial membrane potential of FRDA lymphocytes. In addition, **2** did not inhibit Hsp90 when tested at micromolar concentrations, exhibited no cytotoxicity, and afforded neuroprotection to differentiated SH-SY5Y cells under conditions of Aβ-induced cell toxicity.

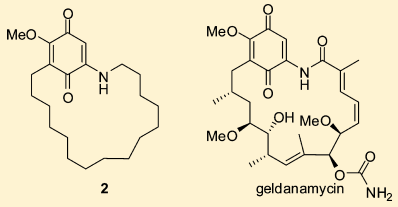

KEYWORDS: *Geldanamycin, oxidative stress, lipid peroxidation, mitochondria*

Mitochondria are cellular organelles that support aerobic respiration essential for the normal functioning of eukaryotic cells.[1,2] In addition to cellular respiration, mitochondria play a vital role in several processes including ATP production, ion homeostasis,[3] and immune response[4] essential for cell survival. Given its important role, mitochondrial dysfunction can have a debilitating effect on human health. Unsurprisingly, mitochondrial damage has been implicated in the genesis and progression of several diseases such as Alzheimer's disease,[5] Parkinson's disease,[5,6] Huntington's disease,[7] and Friedreich's ataxia (FRDA).[8] The disruption of mitochondrial function exposes cells to oxidative damage.[9] The development of novel antioxidants capable of restoring mitochondrial electron transport chain function offers great potential to protect cells from damage caused by mitochondrial dysfunction.

In a recent study, we demonstrated that analogues of natural product **1** (Figure 1), whose structure closely resembles the redox-active quinone core of the natural product geldanamycin,

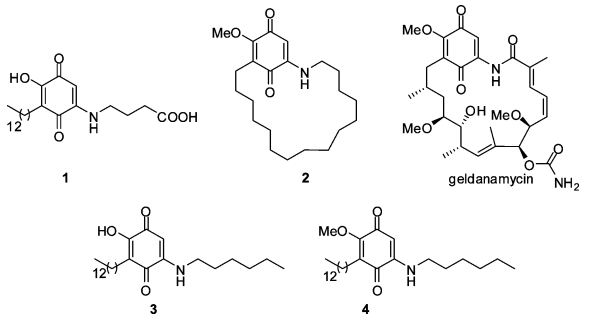

Figure 1. Chemical structures of 5-[*N*-(3-carboxypropyl)amino]-2-hydroxy-3-tridecyl-1,4-benzoquinone natural product (**1**), its derivatives (**2**−**4**), and geldanamycin.

conferred cytoprotection to FRDA lymphocytes in a dose-dependent manner under conditions of induced oxidative stress.[10] Geldanamycin[11] (Figure 1), first isolated from *Streptomyces hygroscopicus*, is a potent inhibitor of chaperone protein Hsp90[12,13] that plays a crucial role in protein refolding[14] and interferes with its ability to regulate several protein kinases.[15,16] The broad antiproliferative activity of geldanamycin against a number of human tumor cell lines[17] has resulted in great interest in the design and synthesis of novel analogues with improved therapeutic profiles or simplified structures.[18−24] In addition to its antiproliferative activity, induction of Hsp70 by geldanamycin has been shown to afford neuroprotection in mice.[25] However, its use for treatment of neurodegenerative diseases is severely limited by its acute cytotoxicity in vivo. In this regard, the synthesis of novobiocin analogues that are C-terminal inhibitors of Hsp90[26] offer much promise, as they afford neuroprotection with no cytotoxicity, apparently due to their induction of Hsp70.[27−29]

Herein, we describe the syntheses of **2**, **3**, and **4** (Figure 1), which are analogues of natural product **1**. Compound **2**, which is a structurally simplified analogue of geldanamycin, was shown to suppress lipid peroxidation (Table 1) and maintain cell viability (Table 2) in a dose-dependent manner at low micromolar concentrations in oxidatively stressed FRDA lymphocytes. In addition, **2** suppressed ROS production (Figure 2) and maintained mitochondrial membrane potential (Figure 3) in cultured FRDA lymphocytes and fibroblasts subjected to oxidative stress. Compound **2** was not cytotoxic (Figure S1, Supporting Information) and protected differentiated SH-SY5Y cells (Figure S2, Supporting Information) against Aβ-induced cell death (Figures 4 and S3, Supporting

Received: May 29, 2013
Accepted: July 25, 2013
Published: July 25, 2013

Table 1. Suppression of Lipid Peroxidation by Nitrogen-Containing 1,4-Benzoquinone Antioxidant Derivatives (2–4) in Cultured FRDA Lymphocytes Treated with Diethyl Maleate (DEM)[a]

	lipid peroxidation scavenging activity (%)		
compd	1 μM	5 μM	10 μM
untreated control[b]	100	100	100
treated control[c]	0	0	0
2[d]	29 ± 4.7	72 ± 6.3	83 ± 2.1
3	2 ± 0.3	27 ± 4.5	38 ± 6.0
4	14 ± 1.3	61 ± 7.5	70 ± 5.8

[a]Lipid peroxidation was detected by utilizing the oxidation-sensitive fatty acid probe C_{11}–BODIPY$^{581/591}$ using FACS. Increased C_{11}–BODIPY-green fluorescence (oxidized form), a measure of intracellular lipid peroxidation, was determined by increasing the median fluorescence intensity of C_{11}–BODIPY-green relative to the untreated control. Results are expressed as % of scavenging activity. Data are expressed as the mean ± SEM (n = 3). [b]No DEM treatment. [c]DEM treatment. [d]Compound **2** was without significant effect on intracellular glutathione concentration at the doses studied.

Table 2. Effect of Nitrogen-Containing 1,4-Benzoquinone Antioxidant Derivatives (2–4) on the Cellular Viability of FRDA Cultured Lymphocytes Treated with Diethyl Maleate (DEM)[a]

	viable cells (%)[b]			
compd	5 μM	2.5 μM	0.5 μM	0.1 μM
2	92 ± 3.5	83 ± 5.4	69 ± 2.3	36 ± 4.3
3	65 ± 5.2	43 ± 4.4	22 ± 2.6	18 ± 2.1
4	80 ± 4.0	66 ± 6.3	50 ± 5.2	20 ± 3.2

[a]Data are expressed as means ± SEM of three independent experiments run in duplicate. [b]The viability of untreated cells was defined as 100%; cells treated with DEM alone had 18 ± 10% viability.

Information). Interestingly, compound **2** did not inhibit Hsp90 (Figure S4, Supporting Information), which may contribute to the cytotoxicity of geldanamycin, further illustrating its potential as a therapeutic agent for relieving oxidative stress.

The synthesis of cyclic geldanamycin analogue **2** is outlined (Scheme 1). The synthesis of **2** began with the alkylation of 1,2,4,5-tetramethoxybenzene (**5**)[10,30,31] with purified 11-bromo-1-undecene to yield **6** in 82% yield. The oxidation of **6** with cerium(IV) ammonium nitrate provided a crude mixture of quinones **7** and **8**, which upon treatment with $HClO_4$–SiO_2[32] led to regioselective demethylation to form hydroxyquinone **8** in 26% yield for two steps.[31] Quinone **8** was coupled with hex-5-en-1-amine hydrochloride (**9**)[33] to form hydroxyquinone **10** in 75% yield. Quinone **10** was methylated to protect the phenolic hydroxyl group, affording methoxyquinone **11** in 74% yield. Compound **11** was subjected to ring closing metathesis in the presence of Grubb's second generation catalyst to yield alkene **12** as a mixture of isomers in 52% yield. The reduction of the alkene by catalytic hydrogenation followed by air oxidation provided **2** in 38% yield for two steps.[34,35] As outlined (Scheme S1, Supporting Information), methoxyquinone **13**[10,31] was treated with hexylamine to yield the corresponding hydroxyquinone **3** in 17% yield. The hydroxyquinone **3** so obtained was methylated with dimethyl sulfate in dry acetone to yield methoxyquinone **4** in 58% yield.

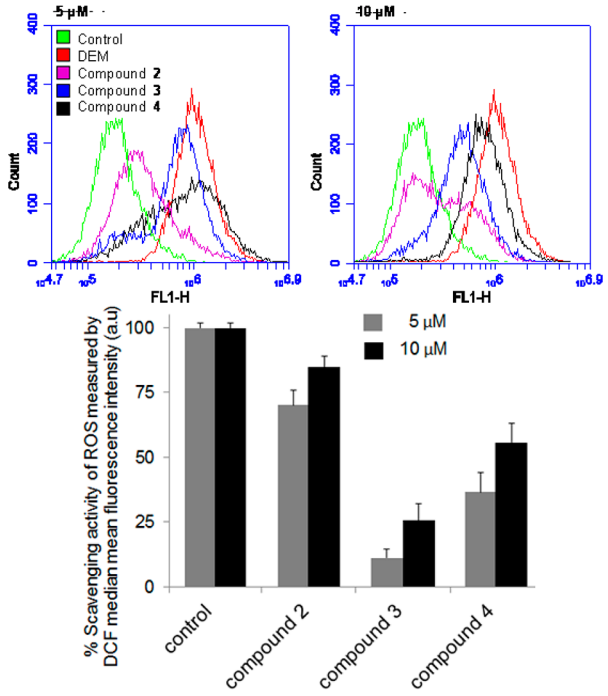

Figure 2. Representative flow cytometric histograms overlay showing ROS production in FRDA lymphocytes. Following pretreatment with the indicated compounds (5 and 10 μM) for 16 h, the cells were treated with 5 mM diethyl maleate (DEM) for 80 min to deplete glutathione. The cells were washed in phosphate-buffered saline and suspended in phosphate-buffered saline containing 20 mM glucose. Cells were loaded with 10 μM dichlorodihydrofluorescein diacetate (DCFH-DA) for 20 min, and the green fluorescence (DCF) was measured by flow cytometry (C6 Accuri, BD Biosciences, San Jose, CA), using a 488 nm excitation laser and the FL1-H channel 530 ± 15 nm emission filter. The figure shows a representative example of three independent experiments. A total of 10,000 events was recorded for each sample and analyzed (C6 Accuri software, BD Biosciences). Increased DCF fluorescence, a measure of intracellular oxidation and ROS production, was determined by a shift in DCF fluorescence to the right on the x-axis of the FACS (fluorescence-activated cell sorting) histogram. The bottom panel shows a bar graph of ROS % scavenging activity. Data are expressed as the mean ± SEM (n = 3).

The ability of **2**, **3**, and **4** to quench lipid peroxidation was evaluated in FRDA lymphocytes (Table 1). The cells were subjected to oxidative stress upon treatment with diethyl maleate (DEM) and shown to have undergone glutathione depletion as described.[36–38] The fatty acid sensitive fluorescent reporter C_{11}–BODIPY$^{581/591}$ (Molecular Probes)[39,40] was used to quantify the extent of lipid peroxidation. Oxidation of the phenylbutadiene moiety of the fluorophore results in a change of fluorescence from red (595 nm) to green (520 nm). Peroxyl radical production was monitored by an increase in C_{11}–BODIPY$^{581/591}$-green (oxidized) fluorescence and determined by flow cytometric analysis. The results show that compound **2** was very effective in suppressing lipid peroxidation at 5 and 10 μM concentrations (72 and 83% suppression, respectively). Methoxyquinone **4** also exhibited significant concentration-dependent suppression of lipid peroxidation (61% and 70% suppression of lipid peroxidation at 5 and 10 μM, respectively), while hydroxyquinone **3** was much less potent (38% suppression at 10 μM concentration).

The ability of **2**, **3**, and **4** to protect cultured FRDA lymphocytes from induced oxidative stress was studied.

dx.doi.org/10.1021/ml400207m | ACS Med. Chem. Lett. 2013, 4, 953–957

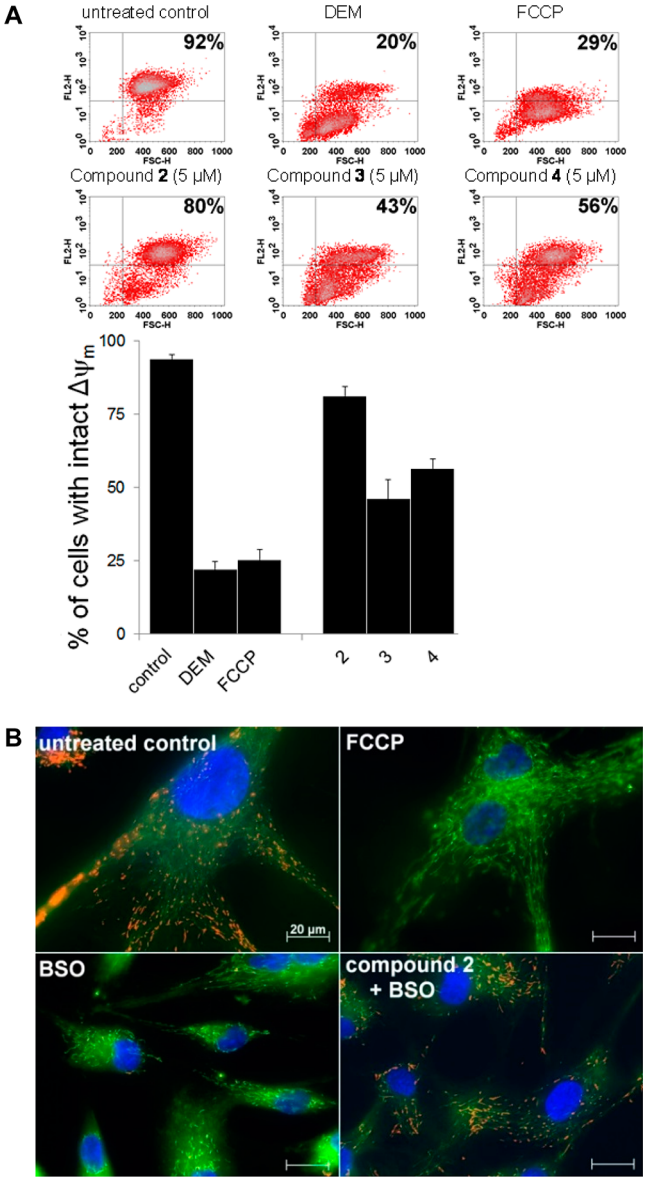

Figure 3. Effect of nitrogen-containing 1,4-benzoquinone derivatives (**2**–**4**) on preservation of mitochondrial membrane potential ($\Delta\psi_m$) of cultured FRDA cells following treatment with the test compounds. (A) Representative flow cytometric two-dimensional color density dot plot analyses of $\Delta\psi_m$ in FRDA lymphocytes stained with TMRM and analyzed using the FL2-H channel as described in the Supporting Information. The percentage of cells with intact $\Delta\psi_m$ is indicated in the top right quadrant of captions. In each analysis, 10,000 events were recorded. Data are expressed as means ± SEM of three independent experiments run in duplicate. The bar graph shows the percentage of cells with intact $\Delta\psi_m$ calculated using CellQuest software. (B) Representative fluorescence microscopy images of JC-1-stained primary FRDA fibroblasts were examined under a Zeiss fluorescent microscope. JC-1 is a dual stain, which can identify high membrane potential through J-aggregates (red fluorescence) and low membrane potential through J-monomers (green fluorescence). When the $\Delta\psi_m$ collapses as a result of glutathione depletion, the reagent (JC-1) no longer accumulates inside the mitochondria; instead, it diffuses throughout the cell cytosol in the monomeric form, which fluoresces green. Hoechst 33342 was used to identify cell nuclei. FCCP (carbonyl cyanide *p*-(trifluoromethyl) phenylhydrazone), a potent uncoupler of mitochondrial oxidative phosphorylation, was run as a control.

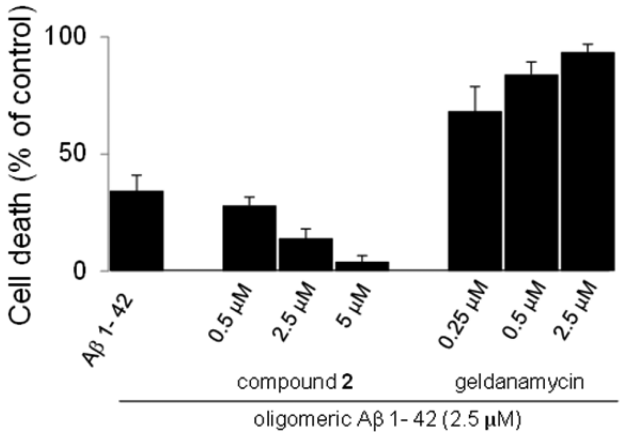

Figure 4. Effect of nitrogen-containing 1,4-benzoquinone **2** and geldanamycin on Aβ 1−42 induced neurotoxicity in differentiated SH-SY5Y cells.

Scheme 1. Synthesis of Compound 2

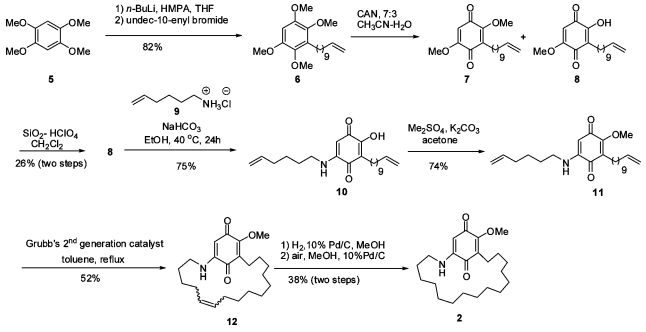

Oxidative stress was induced by treatment with DEM, and cell viability was assessed by trypan blue exclusion. Depletion of glutathione by treatment with DEM has been used to induce oxidative stress in cellular systems by generation of ROS.[37,41,42] As shown (Table 2), the cyclic analogue **2** was most effective, exhibiting 83% and 92% cytoprotection at 2.5 and 5 μM concentrations, respectively. Methoxyquinone **4** afforded greater cytoprotection as compared to hydroxyquinone **3** at 5 μM concentration (80% vs 65%).

The ability of **2**–**4** to suppress ROS production was determined in FRDA lymphocytes by monitoring the fluorescence of ROS-sensitive dye dichlorofluorescein (DCF) in the presence and absence of the test compounds (Figure 2). The cells were subjected to oxidative stress by depleting them of glutathione upon treatment with DEM.[36−38] Intracellular oxidation and ROS production was monitored by an increase in DCF fluorescence and determined by flow cytometry. As shown, **2** effectively suppressed ROS production in stressed cells in a concentration-dependent manner. Compounds **3** and **4** were less effective than **2**.

The ability of the test compounds to maintain mitochondrial membrane potential ($\Delta\psi_m$) under conditions of oxidative stress was studied. $\Delta\psi_m$, an important indicator of cellular function, was measured using two different fluorescent dyes, tetramethylrhodamine methyl ester (TMRM) and 5,5′,6,6′-tetrachloro-1,1′,3,3′-tetraethylbenzimidazolocarbocyanine iodide (JC-1). TMRM is a cell-permeable fluorescent indicator that accumulates in the inner membrane of the mitochondria in a Nernstian manner.[43] There is a direct correlation between $\Delta\psi_m$ across the inner mitochondrial membrane and fluorescence

dx.doi.org/10.1021/ml400207m | ACS Med. Chem. Lett. 2013, 4, 953−957

signal of TMRM. The accumulation of the dye in the mitochondria and the intensity of the signal are direct functions of mitochondrial membrane potential. Loss of membrane potential is indicated by reduction in TMRM red fluorescence. Mitochondrial depolarization using TMRM was detected by flow cytometry. Figure 3A (top panel) illustrates representative two-dimensional density dot plots of TMRM-stained lymphocyte cells showing the percentage of cells with intact $\Delta\psi_m$ (TMRM fluorescence in top right quadrant) vs the percentage of cells with reduced $\Delta\psi_m$ (TMRM fluorescence in bottom left and right quadrants). Figure 3A (bottom panel) shows a bar graph of the percentage (mean ± SEM) of FRDA lymphocytes with intact $\Delta\psi_m$. Treatment with 5 mM DEM resulted in a decrease in the percentage of cells with TMRM fluorescence in the top right quadrant, indicating depolarization of $\Delta\psi_m$ upon DEM treatment. Compound **2** was the most effective at preserving mitochondrial membrane potential at 5 μM concentration (80%). Methoxyquinone **4** was less effective at preserving mitochondrial membrane polarization, while the hydroxyquinone **3** was the least effective at the same concentration (56% and 43%, respectively).

As shown (Figure 3B), these results were further validated using JC-1 dye in primary FRDA fibroblasts treated with buthionine sulfoximine (BSO). BSO induces oxidative stress by inhibiting de novo glutathione synthesis.[44] JC-1 is a lipophilic, cationic dye that selectively enters the mitochondria and undergoes a reversible color change from green to red with the corresponding increase in mitochondrial membrane potential.[45] The dye aggregates in the matrix of healthy energized mitochondria and fluoresces red, while it exhibits green fluorescence in cells with depolarized $\Delta\psi_m$. In untreated FRDA cells and cells treated with 5 μM **2** in addition to 1 mM BSO, the JC-1 dye exhibited red−orange fluorescence (Figure 3B, top left and bottom right quadrants), indicating that **2** preserved mitochondrial membrane potential in the presence of BSO. Treatment with 1 mM BSO prevented accumulation of JC-1 in the mitochondria of cells, resulting in green fluorescence indicating the complete loss of mitochondrial membrane potential (Figure 3B, bottom left quadrant). The mitochondrial chemiosmotic proton gradient ($\Delta\mu H^+$) was dissipated upon treatment with carbonyl cyanide 4-(trifluoromethoxy)phenylhydrazone (FCCP), a commonly used uncoupler of oxidative phosphorylation. The green fluorescence exhibited by cells upon FCCP treatment indicates the depolarization of the mitochondrial inner membrane potential (Figure 3B, top right quadrant). In summary, the above data clearly indicate that **2** effectively preserves the mitochondrial membrane potential under conditions of oxidative stress, an event linked to the disruption of mitochondrial function prior to cell death.

The ability of **2** to protect differentiated SH-SY5Y cells against Aβ-induced cell death was also studied. Compound **2** decreased Aβ 1−42 induced cytotoxicity in a concentration-dependent manner as shown (Figure 4), while geldanamycin actually increased cytotoxicity at comparable concentrations (see, however, ref 28). In addition, compound **2** itself exhibited no cytotoxicity (Figure S1, Supporting Information) and did not inhibit Hsp90, as judged by its lack of effect on the client proteins Her2 and Hsp70 (Figure S4, Supporting Information), the cellular locus of geldanamycin action. This is in agreement with published results showing that the ansa chain plays a key role in the Hsp90 binding and inhibition by geldanamycin[12] and reflects the cytoprotective activity of many benzoquinone analogues.[10,46]

In conclusion, we have synthesized a simple analogue of geldanamycin that was demonstrated to quench lipid peroxidation, confer cytoprotection, and preserve mitochondrial membrane potential in FRDA lymphocytes under conditions of severe induced oxidative stress. Unlike geldanamycin, **2** was not cytotoxic and did not inhibit Hsp90, further suggesting its therapeutic potential for use in the treatment of neurodegenerative diseases.

■ ASSOCIATED CONTENT

Supporting Information

Procedures and characterization data for all compounds, procedures for biochemical assays, and assay data for the effect of **2** on cell viability and Hsp90 client protein abundance. This material is available free of charge via the Internet at http://pubs.acs.org.

■ AUTHOR INFORMATION

Corresponding Author

*(S.M.H.) Tel: 480-965-6625. Fax: 480-965-0038. E-mail: sid.hecht@asu.edu.

Funding

This work was supported by a grant from the Friedreich's Ataxia Research Alliance.

Notes

The authors declare no competing financial interest.

■ REFERENCES

(1) Bras, M.; Queenan, B.; Susin, S. A. Programmed cell death via mitochondria: different modes of dying. *Biochemistry (Moscow)* **2005**, *70*, 231−239.

(2) McBride, H. M.; Neuspiel, M.; Wasiak, S. Mitochondria: more than just a powerhouse. *Curr. Biol.* **2006**, *16*, R551−560.

(3) Cardoso, A. R.; Queliconi, B. B.; Kowaltowski, A. J. Mitochondrial ion transport pathways: role in metabolic diseases. *Biochim. Biophys. Acta, Bioenerg.* **2010**, *1797*, 832−838.

(4) West, A. P.; Shadel, G. S.; Ghosh, S. Mitochondria in innate immune responses. *Nat. Rev. Immunol.* **2011**, *11*, 389−402.

(5) Coskun, P.; Wyrembak, J.; Schriner, S. E.; Chen, H.-W.; Marciniack, C.; LaFerla, F.; Wallace, D. C. A mitochondrial etiology of Alzheimer and Parkinson disease. *Biochim. Biophys. Acta, Gen. Subj.* **2012**, *1820*, 553−564.

(6) McCoy, M. K.; Cookson, M. R. Mitochondrial quality control and dynamics in Parkinson's disease. *Antioxid. Redox Signaling* **2012**, *16*, 869−882.

(7) Mochel, F.; Haller, R. G. Energy deficit in Huntington disease: why it matters. *J. Clin. Invest.* **2011**, *121*, 493−499.

(8) Armstrong, J. S.; Khdour, O.; Hecht, S. M. Does oxidative stress contribute to the pathology of Friedreich's ataxia? A radical question. *FASEB J.* **2010**, *24*, 2152−2163.

(9) Lin, M. T.; Beal, M. F. Mitochondrial dysfunction and oxidative stress in neurodegenerative diseases. *Nature* **2006**, *443*, 787−795.

(10) Madathil, M. M.; Khdour, O. M.; Jaruvangsanti, J.; Hecht, S. M. Synthesis and biological activities of *N*-(3-carboxylpropyl)-5-amino-2-hydroxy-3-tridecyl-1,4-benzoquinone and analogues. *J. Nat. Prod.* **2012**, *75*, 2209−2215.

(11) DeBoer, C.; Meulman, P. A.; Wnuk, R. J.; Peterson, D. H. Geldanamycin, a new antibiotic. *J. Antibiot.* **1970**, *23*, 442−447.

(12) Stebbins, C. E.; Russo, A. A.; Schneider, C.; Rosen, N.; Hartl, F. U.; Pavletich, N. P. Crystal structure of an Hsp90-geldanamycin complex: targeting of a protein chaperone by an antitumor agent. *Cell* **1997**, *89*, 239−250.

(13) Whitesell, L.; Mimnaugh, E. G.; De Costa, B.; Myers, C. E.; Neckers, L. M. Inhibition of heat shock protein HSP90-pp60$^{v\text{-}src}$ heteroprotein complex formation by benzoquinone ansamycins: essential role for stress proteins in oncogenic transformation. *Proc. Natl. Acad. Sci. U.S.A.* **1994**, *91*, 8324−8328.
(14) Schneider, C.; Sepp-Lorenzino, L.; Nimmesgern, E.; Ouerfelli, O.; Danishefsky, S.; Rosen, N.; Hartl, F. U. Pharmacologic shifting of a balance between protein refolding and degradation mediated by Hsp90. *Proc. Natl. Acad. Sci. U.S.A.* **1996**, *93*, 14536−14541.
(15) An, W. G.; Schulte, T. W.; Neckers, L. M. The heat shock protein 90 antagonist geldanamycin alters chaperone association with p210$^{bcr\text{-}abl}$ and v-src proteins before their degradation by the proteasome. *Cell Growth Differ.* **2000**, *11*, 355−360.
(16) Schulte, T. W.; Blagosklonny, M. V.; Ingui, C.; Neckers, L. Disruption of the Raf-1-Hsp90 molecular complex results in destabilization of Raf-1 and loss of Raf-1-Ras association. *J. Biol. Chem.* **1995**, *270*, 24585−24588.
(17) Whitesell, L.; Shifrin, S. D.; Schwab, G.; Neckers, L. M. Benzoquinonoid ansamycins possess selective tumoricidal activity unrelated to *src* kinase inhibition. *Cancer Res.* **1992**, *52*, 1721−1728.
(18) Clevenger, R. C.; Blagg, B. S. J. Design, synthesis, and evaluation of a radicicol and geldanamycin chimera, radamide. *Org. Lett.* **2004**, *6*, 4459−4462.
(19) Wang, M.; Shen, G.; Blagg, B. S. J. Radanamycin, a macrocyclic chimera of radicicol and geldanamycin. *Bioorg. Med. Chem. Lett.* **2006**, *16*, 2459−2462.
(20) Kuduk, S. D.; Zheng, F. F.; Sepp-Lorenzino, L.; Rosen, N.; Danishefsky, S. J. Synthesis and evaluation of geldanamycin-estradiol hybrids. *Bioorg. Med. Chem. Lett.* **1999**, *9*, 1233−1238.
(21) Kuduk, S. D.; Harris, C. R.; Zheng, F. F.; Sepp-Lorenzino, L.; Ouerfelli, Q.; Rosen, N.; Danishefsky, S. J. Synthesis and evaluation of geldanamycin-testosterone hybrids. *Bioorg. Med. Chem. Lett.* **2000**, *10*, 1303−1306.
(22) Zheng, F. F.; Kuduk, S. D.; Chiosis, G.; Munster, P. N.; Sepp-Lorenzino, L.; Danishefsky, S. J.; Rosen, N. Identification of a geldanamycin dimer that induces the selective degradation of HER-family tyrosine kinases. *Cancer Res.* **2000**, *60*, 2090−2094.
(23) McErlean, C. S. P.; Proisy, N.; Davis, C. J.; Boland, N. A.; Sharp, S. Y.; Boxall, K.; Slawin, A. M. Z.; Workman, P.; Moody, C. J. Synthetic ansamycins prepared by a ring-expanding Claisen rearrangement. Synthesis and biological evaluation of ring and conformational analogues of the Hsp90 molecular chaperone inhibitor geldanamycin. *Org. Biomol. Chem.* **2007**, *5*, 531−546.
(24) Kitson, R. R. A.; Chang, C.-H.; Xiong, R.; Williams, H. E. L.; Davis, A. L.; Lewis, W.; Dehn, D. L.; Siegel, D.; Roe, S. M.; Prodromou, C.; Ross, D.; Moody, C. J. Synthesis of 19-substituted geldanamycins with altered conformations and their binding to heat shock protein Hsp90. *Nat. Chem.* **2013**, *5*, 307−314.
(25) Shen, H.-Y.; He, J.-C.; Wang, Y.; Huang, Q.-Y.; Chen, J.-F. Geldanamycin induces heat shock protein 70 and protects against MPTP-induced dopaminergic neurotoxicity in mice. *J. Biol. Chem.* **2005**, *280*, 39962−39969.
(26) Marcu, M. G.; Chadli, A.; Bouhouche, I.; Catelli, M.; Neckers, L. M. The heat shock protein 90 antagonist novobiocin interacts with a previously unrecognized ATP-binding domain in the carboxyl terminus of the chaperone. *J. Biol. Chem.* **2000**, *275*, 37181−37186.
(27) Ansar, S.; Burlison, J. A.; Hadden, M. K.; Yu, X. M.; Desino, K. E.; Bean, J.; Neckers, L.; Audus, K. L.; Michaelis, M. L.; Blagg, B. S. J. A non-toxic Hsp90 inhibitor protects neurons from Aβ-induced toxicity. *Bioorg. Med. Chem. Lett.* **2007**, *17*, 1984−1990.
(28) Lu, Y.; Ansar, S.; Michaelis, M. L.; Blagg, B. S. J. Neuroprotective activity and evaluation of Hsp90 inhibitors in an immortalized neuronal cell line. *Bioorg. Med. Chem.* **2009**, *17*, 1709−1715.
(29) Blagg, B.; Michaelis, M. L.; McIntosh, M. *Preparation of novobiocin analogs useful for the treatment and/or prevention of neurodegenerative disorders, autoimmune disorders, and as antitumor agents*. U. S. Patent 7,622,451, 24 Nov 2009.
(30) Matsumoto, M.; Kobayashi, K.; Hotta, Y. Acid-catalyzed oxidation of benzaldehydes to phenols by hydrogen peroxide. *J. Org. Chem.* **1984**, *49*, 4740−4741.
(31) Poigny, S.; Guyot, M.; Samadi, M. Total synthesis of maesanin and analogues. *Tetrahedron* **1998**, *54*, 14791−14802.
(32) Chakraborti, A. K.; Gulhane, R. Perchloric acid adsorbed on silica gel as a new, highly efficient, and versatile catalyst for acetylation of phenols, thiols, alcohols, and amines. *Chem. Commun.* **2003**, 1896−1897.
(33) Gagne, M. R.; Stern, C. L.; Marks, T. J. Organolanthanide-catalyzed hydroamination. A kinetic, mechanistic, and diastereoselectivity study of the cyclization of *N*-unprotected amino olefins. *J. Am. Chem. Soc.* **1992**, *114*, 275−294.
(34) Luly, J. R.; Rapoport, H. Routes to mitomycins. An improved synthesis of 7-methoxymitosene using palladium catalysis. *J. Org. Chem.* **1984**, *49*, 1671−1672.
(35) Shen, G.; Wang, M.; Welch, T. R.; Blagg, B. S. J. Design, synthesis, and structure−activity relationships for chimeric inhibitors of Hsp90. *J. Org. Chem.* **2006**, *71*, 7618−7631.
(36) Armstrong, J. S.; Jones, D. P. Glutathione depletion enforces the mitochondrial permeability transition and causes cell death in HL60 cells that overexpress Bcl-2. *FASEB J.* **2002**, *16*, 1263−1265.
(37) Armstrong, J. S.; Whiteman, M.; Rose, P.; Jones, D. P. The coenzyme Q_{10} analog decylubiquinone inhibits the redox-activated mitochondrial permeability transition: Role of mitochondrial respiratory complex III. *J. Biol. Chem.* **2003**, *278*, 49079−49084.
(38) Khdour, O.; Lu, J.; Hecht, S. M. An acetate prodrug of a pyridinol-based vitamin E analogue. *Pharm. Res.* **2011**, *28*, 2896−2909.
(39) Pap, E. H. W.; Drummen, G. P. C.; Winter, V. J.; Kooij, T. W. A.; Rijken, P.; Wirtz, K. W. A.; Op den Kamp, J. A. F.; Hage, W. J.; Post, J. A. Ratio-fluorescence microscopy of lipid oxidation in living cells using C11-BODIPY$^{581/591}$. *FEBS Lett.* **1999**, *453*, 278−282.
(40) Drummen, G. P. C.; van Liebergen, L. C. M.; Op den Kamp, J. A. F.; Post, J. A. C11-BODIPY$^{581/591}$, an oxidation-sensitive fluorescent lipid peroxidation probe: (micro)spectroscopic characterization and validation of methodology. *Free Radical Biol. Med.* **2002**, *33*, 473−490.
(41) Miccadei, S.; Kyle, M. E.; Gilfor, D.; Farber, J. L. Toxic consequence of the abrupt depletion of glutathione in cultured rat hepatocytes. *Arch. Biochem. Biophys.* **1988**, *265*, 311−320.
(42) Tirmenstein, M. A.; Nicholls-Grzemski, F. A.; Zhang, J. G.; Fariss, M. W. Glutathione depletion and the production of reactive oxygen species in isolated hepatocyte suspensions. *Chem.-Biol. Interact.* **2000**, *127*, 201−217.
(43) Ehrenberg, B.; Montana, V.; Wei, M. D.; Wuskell, J. P.; Loew, L. M. Membrane potential can be determined in individual cells from the Nernstian distribution of cationic dyes. *Biophys. J.* **1988**, *53*, 785−794.
(44) Griffith, O. W.; Meister, A. Potent and specific inhibition of glutathione synthesis by buthionine sulfoximine (*S-n*-butyl homocysteine sulfoximine). *J. Biol. Chem.* **1979**, *254*, 7558−7560.
(45) Smiley, S. T.; Reers, M.; Mottola-Hartshorn, C.; Lin, M.; Chen, A.; Smith, T. W.; Steele, G. D.; Chen, L. B. Intracellular heterogeneity in mitochondrial membrane potentials revealed by a J-aggregate-forming lipophilic cation JC-1. *Proc. Natl. Acad. Sci. U.S.A.* **1991**, *88*, 3671−3675.
(46) Fash, D. M.; Khdour, O. M.; Sahdeo, S. J.; Goldschmidt, R.; Jaruvangsanti, J.; Dey, S.; Arce, P. M.; Collin, V. C.; Cortopassi, G. A.; Hecht, S. M. Effects of alkyl side chain modification of coenzyme Q_{10} on mitochondrial respiratory chain function and cytoprotection. *Bioorg. Med. Chem.* **2013**, *21*, 2346−2354.